



Enzyme and Thermo Dual-stimuli Responsive DOX Carrier Based on PNIPAM Conjugated Mesoporous Silica

Seyyed Mostafa Ebrahimi¹, Mahdieh Karamat Iradmousa¹, Mahtab Rashed¹, Yousef Fattahi^{2,3}, Yalda Hosseinzadeh Ardakani³, Saeed Bahadorikhalili⁴, Reza Bafkary², Mohammad Erfan¹, Rassoul Dinarvand^{2,3,*} and Arash Mahboubi^{1,**}

¹Department of Pharmaceutics, School of Pharmacy, Shahid Beheshti University of Medical Sciences, Tehran, Iran

²Nanotechnology Research Center, Faculty of Pharmacy, Tehran University of Medical Sciences, Tehran, Iran

³Department of Pharmaceutical Nanotechnology, Faculty of Pharmacy, Tehran University of Medical Sciences, Tehran, Iran

⁴Department of Electronic Engineering, Rovira i Virgili University, Tarragona, Spain

*Corresponding author: Nanotechnology Research Center, Faculty of Pharmacy, Tehran University of Medical Sciences, Tehran, Iran. Email: dinarvand@tums.ac.ir

**Corresponding author: Department of Pharmaceutics, School of Pharmacy, Shahid Beheshti University of Medical Sciences, Tehran, Iran. Email: a.mahboubi@sbmu.ac.ir

Received 2021 December 09; Revised 2022 February 07; Accepted 2022 March 16.

Abstract

Background: Stimuli-responsive drug delivery systems have been proven to be a promising strategy to enhance tumor localization, overcome multidrug resistance (MDR), and reduce the side effects of chemotherapy agents.

Objectives: In this study, a temperature and redox dual stimuli-responsive system using mesoporous silica nanoparticles (MSNs) for targeted delivery of doxorubicin (DOX) was developed.

Methods: Mesoporous silica nanoparticles were capped with poly(N-isopropylacrylamide) (PNIPAM), a thermo-sensitive polymer, with atom transfer radical polymerization (ATRP) method, via disulfide bonds (DOX-MSN-S-S-PNIPAM) to attain a controlled system that releases DOX under glutathione-rich (GSH-rich) environments and temperatures above PNIPAM's lower critical solution temperature (LCST). Morphological and physicochemical properties of the nanoparticles were indicated using transmission electron microscopy (TEM), dynamic light scattering (DLS), energy-dispersive X-ray spectroscopy (EDS), thermogravimetric analysis (TGA), differential scanning calorimetry (DSC), and Brunauer-Emmett-Teller (BET). The drug release tests were performed at 25°C and 41°C in the absence and presence of the DTT, and the obtained results confirmed the synergic effect of temperature and reductive agent on a dual responsive release profile with a 73% cumulative release at 41°C and reductive environment during 240 min.

Results: The average loaded drug content and encapsulation efficacy were reported as 42% and 29.5% at the drug: nanoparticle ratio of 1.5: 1. In vitro cytotoxicity assays on MCF-7 cell lines indicated significant viability decreased in cells exposed to DOX-MSN-S-S-PNIPAM compared to the free drug (DOX).

Conclusions: Based on the results, DOX-MSN-S-S-PNIPAM has shown much more efficiency with stimuli-responsive properties in comparison to DOX on MCF-7 cancer cell lines.

Keywords: ATRP Polymerization, Drug Delivery, Stimuli-Responsive, Cancer, Nanoparticles

1. Background

Doxorubicin, an anticancer agent of the anthracycline family, is one of the most popular anti-neoplastic drugs used for decades in the treatment of various cancer tumors, particularly breast and ovarian, leukemia, and lymphoma (1). Nevertheless, doxorubicin (DOX) presents many unfavorable side effects due to its low specificity. Some of these side effects are induced vomiting with nausea, mucositis, myelosuppression, and dose-dependent cardiotoxicity. Cardiotoxicity can result in irreversible heart failure. Also, using the DOX regimen presents acquired multidrug-resistant (MDR) due to several biological

mechanisms upon repeated chemotherapy cycles (2, 3).

Multidrug resistance (MDR) is a multifactorial phenomenon and mostly mainly occurs due to various mechanisms with several cellular pathways, for instance, mutations in oncogenes (4) and increased release of the drug outside the cells via ATP-binding cassette (ABC) transporters. P-glycoprotein (P-gp) is a member of the ABC family responsible for carrying DOX out of the cell (5).

Nowadays, to cope with these challenges, controlled drug delivery systems (CDDS) have attracted attention due to improving chemotherapeutics' performance, including decreasing dose frequency, improving drug efficacy,

and reducing side effects (6).

Among various drug delivery systems, organic-based nanocarriers have exhibited great successful systems. These systems are faced with a few disadvantages, such as entrapped drug leakage and premature degradation of the active agent. On the other hand, inorganic material-based nanocarriers can be used as promising alternative drug delivery systems (7).

Since the first discovery of Mobil Composition of Matter No. 41 (MCM-41) materials in 1992 (8, 9), mesoporous silica nanoparticles (MSNs) have been highlighted as a promising alternative drug carrier platform. It can be an efficient drug carrier due to tuneable pore diameter and particle sizes (2 - 10 nm), abundant surface functionalization sites ($> 1000 \text{ m}^2/\text{g}$) (10), superior biocompatibility (11), reproducible synthesis procedure (12), and versatile chemistry for further functionalization (6, 13).

Furthermore, MSNs can accumulate preferably at the tumor site and improve the “enhanced permeability and retention” (EPR) effect. As a result, they have been widely evaluated for cancer diagnosis and therapy and other biomedical applications (14).

Premature drug leakage from nanoparticles in uncoated MSNs could lead to fast drug release (15). To solve these drawbacks, reversible capping was applied to the surface pores of MSNs, improving drug delivery capability. Moreover, improved controlled drug release could be provided by applying one or more stimuli to the cap structure (16).

Stimuli-responsive DDS has developed with the ability to respond quickly to different external (light, ultrasound, magnetic field) or intra-tumoral (redox, pH, enzymes, temperature) initiatives (17). These systems cannot only achieve better control over drug release but also maintain the effective concentration of drugs in targeted tissues for a longer period of time. Temperature is one of the most frequently used factors in stimuli-responsive systems. Body temperature is locally or generally affected by different conditions and environments. Moreover, the temperature is an easily controlled element during various experiments. These attributes make the temperature a convenient factor for designing responsive drug delivery systems (18, 19).

For more than 20 years, numerous researchers have been intrigued by chipping away at the thermo-responsive hydrogels and polymers (20). One of the most studied thermosensitive polymers is poly(N-isopropyl acrylamide) (PNIPAM). It was firstly synthesized in the 1950s (21). Poly(N-isopropylacrylamide) is characterized by an “on” (adhesive) and “off” (non-adhesive) states. It can indirectly change bio-adhesiveness via extending the chain through hydration below the lower critical solution temperature

(LCST) of 32°C and collapsing conformation above LCST. These conditions are known as “random coil” and “globular” conformations. Having an LCST nearby human body temperature makes PNIPAM suitable for assembling with MSNs as nanocarriers (18, 22).

The grafting of PNIPAM on the silica nanoparticles can be fabricated by the atom transfer radical polymerization (ATRP) technique. Atom transfer radical polymerization is a living radical polymerization that relies on the equilibrium between dormant and active chains. This method allows narrow molecular weight dispersity of synthesized polymers, predictable chain length, and defined chain-ends (23, 24).

In addition to temperature, redox-responsive behavior is an excellent choice for a better controlled drug delivery. It was demonstrated that various concentrations of glutathione (GSH) are present in different body sites, as it was found at approximately 10 mM in the intracellular matrix and below 0.02 mM in the plasma. Furthermore, in several studies, GSH is located in tumor cells at level 4 orders of magnitude or (at least) higher than normal cells. So, the disulfide bonds are relatively stable in extracellular fluid, whereas they can be cleaved in other environments (25, 26).

Once the drug-loaded MSN-S-S-PNIPAM reached tumor sites, the PNIPAM chain in the outer layer would be collapsed first and then removed to release more DOX after decomposition of the disulfide cross-linker in the presence of glutathione.

2. Objectives

This study aimed to design and construct a chemohyperthermia drug delivery platform consisting of thermosensitive PNIPAM as a gatekeeper of release and MSNs as drug containers. The release studies were performed to approve the dual stimuli-responsive character of the designed MSNs. Further studies were conducted to investigate the different characterization of the nanocarriers.

3. Methods

3.1. Material

Doxorubicin hydrochloride (2 mg/mL) was purchased from Korea United Pharm Inc. (Chungnam, Korea). Cetyltrimethylammonium bromide (CTAB), tetraethylorthosilicate (TEOS), (3-glycidyloxypropyl)trimethoxysilane (GPTMS), cystamine, 3-(4,5-dimethylthiazol-2-yl)-2,5-diphenyl tetrazolium bromide (MTT), 2-bromoisobutyryl bromide (BIBB),

dithiothreitol (DTT), ammonium nitrate (NH_4NO_3), hydrochloric acid (HCl), sodium hydroxide (NaOH), ethanol, triethanolamine (TEA), and chloroform provided by Sigma Aldrich, USA. Deionized water was used for the synthesis purified with the Milli-Q system. All the chemicals were utilized without further purification.

3.2. Methods

3.2.1. Synthesis of Mesoporous Silica Nanoparticles

The surfactant templating method was used to synthesize MSNs according to the Nohavane method (27). Simply, 1.0 g CTAB as the template was dissolved in 480 mL deionized water containing 280 mg NaOH. The mixture was stirred for 15 min at 80°C. Then, 5.36 mL TEOS as a precursor was added drop-wise to the mixed solution under stirring (Heidolph, 400 rpm) for 2 h. The synthesized white precipitate was centrifuged for 15 min at 16000 rpm (Sigma), washed with 50: 50 (v/v) double deionized water and ethanol three times, and freeze-dried for 24 h.

For template extraction, 600 mg NH_4NO_3 was subsequently added to absolute ethanol solutions of MSN, refluxed for 24 h under an N_2 atmosphere, and washed three times with deionized water. Then 5 mL of HCl 37% was added to the MSNs solutions resulting from the previous step under similar conditions.

3.2.2. Functionalization of Mesoporous Silica Nanoparticles with (3-Glycidyloxypropyl)trimethoxysilane

In order to surface modification of MSNs by GPTMS, 700 mg of MSNs was dispersed into absolute ethanol, then 1.5 mL GPTMS (5.5 mM) was added under an N_2 atmosphere for 24 h. The process was conducted with the reflux system (Figure 1).

3.2.3. Introduction of Disulfide Cysteamine Groups (Mesoporous Silica Nanoparticle (MSN)-S-S-NH₂)

Introducing the disulfide bond onto the MSNs was done via cystamine dihydrochloride. Mesoporous silica nanoparticles-GPTMS and cystamine were dispersed in anhydrous ethanol (the molar ratio is about 2: 1). Afterward, the solution of MSN-GPTMS was added drop-wise to cystamine. The mixture was refluxed for 24 h to form the sulfide band by the reaction of the epoxide group of GPTMS with cystamine.

3.2.4. Producing Atom Transfer Radical Polymerization Initiators on Mesoporous Silica Nanoparticle

The ATRP initiators containing reductive disulfide bonds were prepared by a covalent connection between BIBB and MSN-S-S-NH₂. Briefly, MSN-S-S-NH₂ was dispersed

in dichloromethane, followed by the addition of TEA. 2-bromoisobutyryl bromide dissolved in dichloromethane was added drop-wise to the aforementioned solution in an ice-acetone bath, then permitted the mixture to stir for 4 h at 5°C under N_2 atmosphere. The solution was stirred for the next 24 h at room temperature. After centrifuging, washing, and drying, the finished product was obtained (MSN-S-S-Br).

3.2.5. Synthesis of Mesoporous Silica Nanoparticle (MSN)-S-S-Poly(N-isopropylacrylamide) (PNIPAM)

The PNIPAM was covalently anchored to the surface of the MSNs by using MSN-S-S-Br as an initiator (28, 29). A typical procedure is as follows: A ratio of 2.44 g (N-isopropylacrylamide)-co-methacrylic acid (NIPAM), 21 μL of PMDETA as a ligand, and 7 mL of methanol/deionized water (1: 1) were placed into a 20 mL dry vial. Twelve mg CuBr and 16 mg CuBr_2 (as catalysts) were placed into another vial. All the pre-sealed systems were exposed to nitrogen gas for 30 min. Subsequently, the monomer-ligand solution was added to a rubber plug sealed vial containing 162 mg MSN-S-S-Br with a glass syringe. The polymerization reaction started with adding the catalysts, and the color of the solution changed to blue. The reaction continued at room temperature with stirring for 24 h. The resulting MSN-S-S-PNIPAM was centrifuged and rinsed repeatedly with ethanol and deionized water.

3.2.6. Physicochemical and Morphological Characterization

The characterization and morphology study of functionalized MSNs were performed using transmission electron microscopy (TEM) images captured from Zeiss Leo 906. The size distribution of nanocarriers was determined by dynamic light scattering (DLS) (Malvern Instruments, Malvern, UK). To examine the long-range order of porous material, X-ray diffraction (XRD) patterns were recorded by Bruker D8FOCUS X-ray diffractometer. Fourier transform infrared spectra (FTIR) were measured in the region of 400 - 4000 cm^{-1} with a spectrometer (Bruker, Germany) to inspect the structure and major functional groups of MSNs. The chemical composition of samples was analyzed by energy-dispersive X-ray spectroscopy (EDS) analysis.

The thermal stability of nanoparticles was evaluated by thermogravimetric analyses (TGA) using the heating rate of 10°C.min⁻¹ under a nitrogen atmosphere (TGA Q50 V6.3 Build 189).

Ultra-sensitive differential scanning calorimetry (US-DSC) analysis was applied to study phase transition changes of the thermosensitive layer of nanoparticles (0.1% (W/V) MSN-S-S-PNIPAMs aqueous solution) applying a heating rate of 1°C.min⁻¹ from 15°C to 70°C (Micro Cal Inc.).

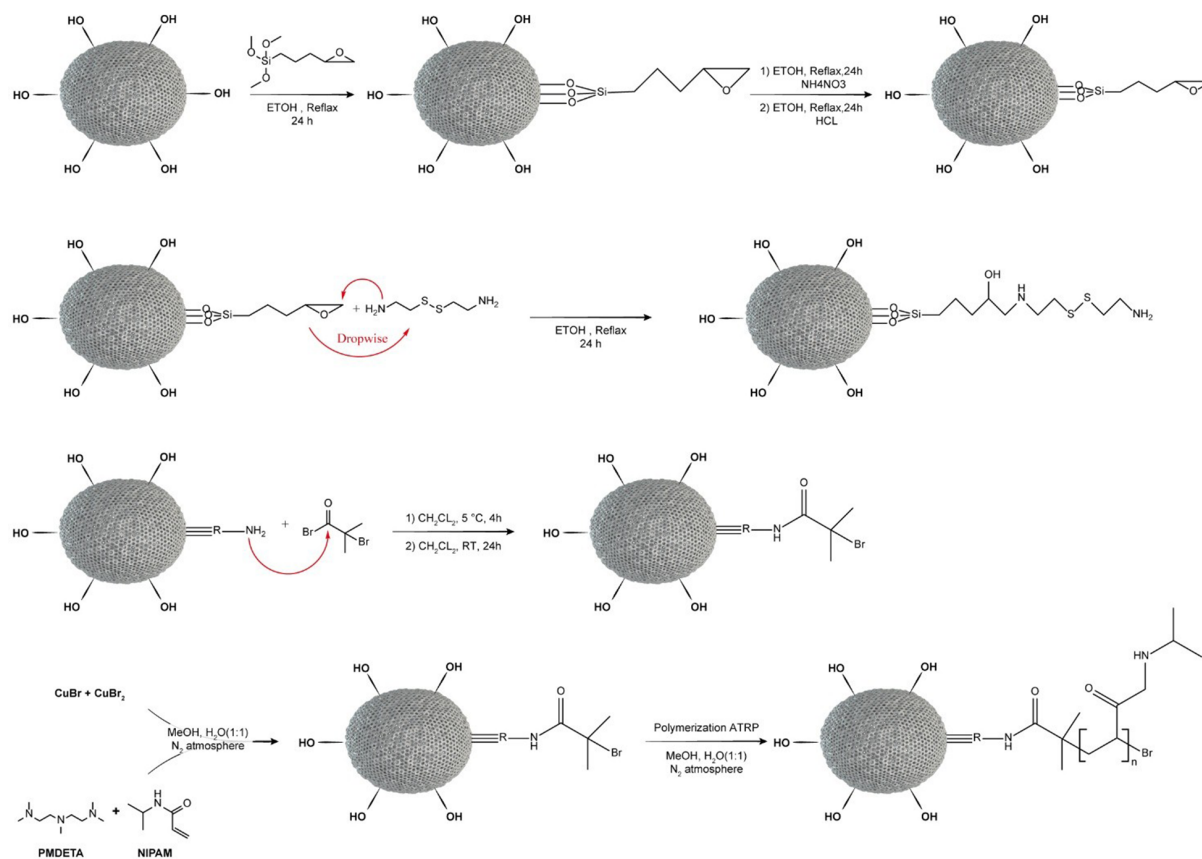


Figure 1. Synthesis steps of mesoporous silica nanoparticle (MSN)-S-S-Poly(N-isopropylacrylamide) (PNIPAM)

N_2 adsorption-desorption isotherms were evaluated using a surface area and porosity analyzer (BELSORP-miniII Guo2019).

3.2.7. Drug Loading and In Vitro Release

Drug loading and in vitro release were evaluated by the method described by Huang et al. (16) Briefly, 10 mg of MSN-S-S-PNIPAMs was dispersed in 20 mL PBS (pH = 7.4). One milliliter of various aqueous concentrations of DOX (5, 10, 15, and 20 mg/mL) was prepared and stirred with the nanocarriers at 25°C for 24 h in a dark place.

Finally, after the loaded nanoparticles of DOX-MSN-S-S-PNIPAM were separated with a magnet, the product was rinsed several times with deionized water to remove the unbound drugs. The content of free DOX was estimated using the UV absorbance of the supernatants measured at 490 nm using the calibration curve. The drug loading content (DL) and the drug encapsulation efficacy (EE) were determined as follows (16):

$$DL = \frac{\text{Mass of loaded DOX}}{\text{Mass of nanoparticles}} \times 100 \quad (1)$$

$$EE = \frac{\text{Mass of loaded DOX}}{\text{Total dosage of feeding DOX}} \times 100 \quad (2)$$

The release behavior of DOX was performed in the presence or absence of DTT (20 mM) using a dialysis bag (12 kDa molecular weight cut-off). Besides, to obtain the phase transition temperature of the MSN-S-S-PNIPAM, the experiment was carried out at 25°C and 41°C.

Ten milligrams of DOX-loaded nanoparticles were suspended in 20 mL of phosphate-buffered saline (PBS, 40 mM, pH = 7.4) and set in a dialysis bag with stirring at 90 rpm. Three milliliters of release medium were taken at defined time intervals and replaced with equal fresh pre-warmed PBS. The concentration of DOX was determined by UV measurement, as mentioned before. Each experiment was performed in triplicate, and the mean \pm SD of the results was reported.

3.2.8. In Vitro Cytotoxicity Assays

Nanoparticle cytotoxicity studies on Michigan Cancer Foundation-7 (MCF-7) cells were assessed by the MTT test.

Michigan Cancer Foundation-7 cells were cultured in 96-well plates (1×10^4 cells/well) for 24 h in a 5% CO₂ humidified atmosphere. After 24 h, the old medium of each well was replaced with the fresh medium containing free DOX or DOX-loaded nanocarriers with the same concentrations. After incubation for 48 h, 20 μ L of MTT (5 mg/mL, PBS) solution was added, and the cells were further incubated at 37°C for 4 h. The medium was sucked out, and 150 μ L of dimethyl sulfoxide (DMSO) was added to each well. After mixing, the optical density values of the samples are measured at 570 nm (30).

4. Results and Discussion

4.1. Design and Preparation of Mesoporous Silica Nanoparticle (MSN)-S-S-Poly(N-isopropylacrylamide) (PNIPAM)

Like many other chemotherapeutic agents, low permeability (DOX class III biopharmaceutical classification system (BCS)) and acute systemic toxicity have limited the efficacy and usage of DOX. To overcome these disadvantages and early release of DOX, DOX was loaded to MSNs and linked to thermosensitive polymer and disulfide bands to control the release via temperature, and redox dual modulated responsive system. As proof of concept, the synthetic process of MSN-S-S-PNIPAM is shown in Figure 2. Mobil Composition of Matter No. 41 was firstly synthesized by the surfactant templating method.

In this method, TEOS was utilized as a silicon source, and CTAB, a cationic surfactant, was utilized as a template to fabricate pore structures in an alkaloid environment. In order to prevent size changes by NaOH, the final product was washed with deionized water and ethanol. Then, the process of removing the template was done. Compared with other methods of removing CTAB, the previously mentioned method did not increase the particle size of MSNs.

Afterward, to get the reductive MSN-S-S-NH₂, MSNs were functionalized with GPTMS, and the MSNs-GPTMS reacted with cystamine.

To achieve dual responsive targeted drug release, the MSN-S-S-NH₂ was covalently bound to NIPAM polymer via ATRP technique. 2-bromoisobutyryl bromide was used as an ATRP initiator. The presence of the -Br group in the EDS has been performed by the BIBB binding to MSN-S-S-NH₂. The synthesis steps of MSN-S-S-PNIPAM are presented in Figure 1.

Energy-dispersive X-ray spectroscopy, FTIR, and TEM analyses were done to confirm whether each step modification on MSNs was rightly completed. Finally, the smart delivery system is produced after loading DOX into the nanocarriers by physical adsorption.

4.2. Morphology and Size Analysis of Nanoparticles

4.2.1. Fourier Transform Infrared Spectra Analysis

Figure 3 shows the FTIR spectra of different steps of the prepared nanoparticles. The strong peak around 1088 cm⁻¹ was attributed to the stretching of the Si-O-Si band. The presence of two sharp peaks at 2859 and 2974 cm⁻¹ corresponds to the C-H stretching band of the CTAB. After the removal of the surfactant, the peaks disappeared. After the modification of MSNs with cystamine, the peaks around ~1346 cm⁻¹ were implied to stretching of C-N bonds, whereas the peaks at 1474 cm⁻¹ and 1554 cm⁻¹ were shown as the N-H bands of the NH₂ group.

Vibration bands at 1657 and 1589 cm⁻¹ are correlated to amide I and amide II bands (N-H stretching). Also, in 1492 cm⁻¹, the amide III bands can be distinguished. Furthermore, the peaks about 1380 and 2974 cm⁻¹ raised due to -CH(CH₃)₂ and -CH₃. All these data indicate the successful attaching of PNIPAM polymer to the surface of mesoporous silica nanoparticles.

Zeta potential measurements evaluated the surface charge of prepared samples. The zeta potential of primary MSNs was about +25 mV. After the addition of GPTMS, the zeta potential changed to +16 mV because of decreasing in hydroxyl groups of the MSN surface. The zeta potential altered to -20 mV after the CTAB removal process. The zeta potential of modified MSN with cystamine returned to highly positive voltage again (around +20 mV), which could be due to the presence of -NH₂.

4.2.2. Energy-Dispersive X-Ray Spectroscopy Analysis

Energy-dispersive X-ray spectroscopy analysis was used for the elemental characterization of the samples at each step of modifications. To investigate the complete removal of the CTAB, EDS analysis was conducted, and the result showed only the silicon and oxygen peaks, as similar outcomes obtained by FTIR.

After the modification with cystamine, the EDS result contains 1.04% nitrogen, 5.38% carbon, and 0.98% sulfur in addition to oxygen and silicon. Furthermore, the bromine peak at MSN-BIBB analysis confirmed the successful attachment of -Br to the mesoporous nanoparticles.

4.2.3. X-Ray Diffraction Analysis

The XRD pattern of MSN is depicted in Figure 4. As described before, the synthesized mesoporous silica for using CTAB is MCM-41. The XRD pattern (1 0 0), (1 1 0), and (2 0 0) proved to prepare a highly ordered hexagonal structure of mesoporous silica structure (31).

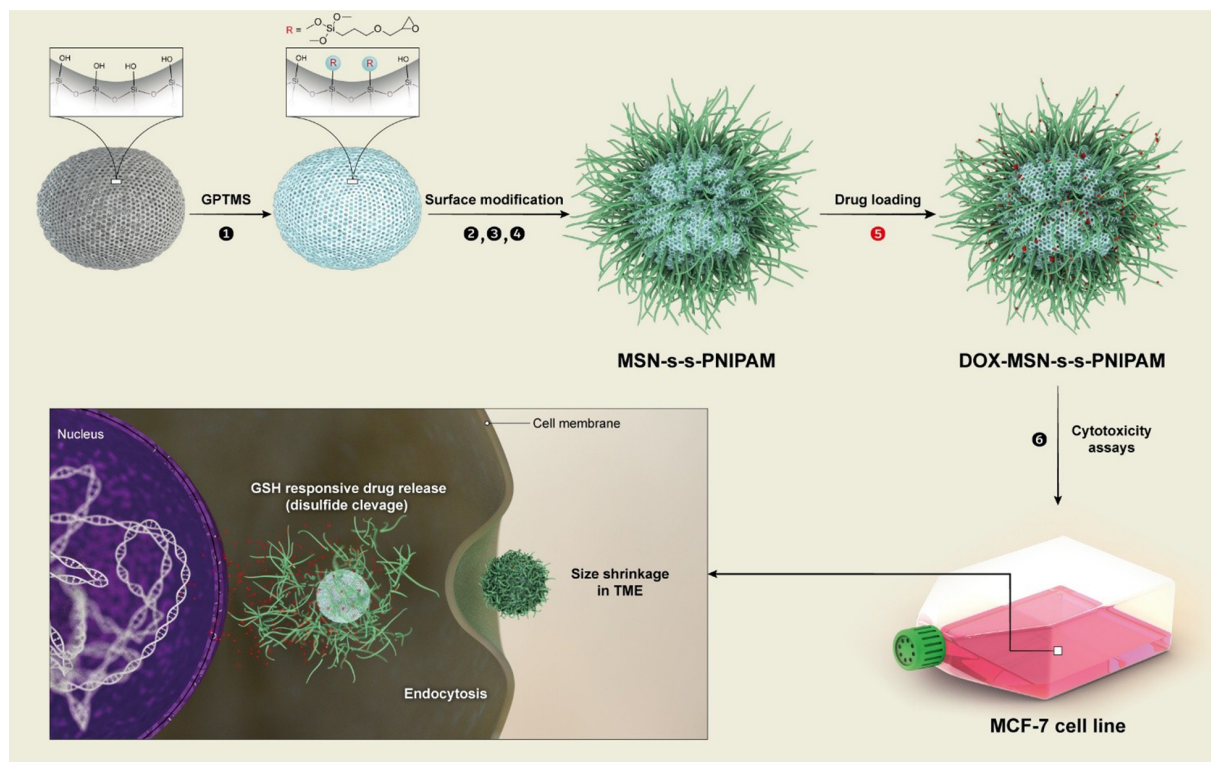


Figure 2. A schematic pattern of synthesizing stimuli-responsive mesoporous silica and cellular uptake and doxorubicin (DOX) release of mesoporous silica nanoparticle (MSN)-S-S-poly(N-isopropylacrylamide) (PNIPAM). (1) (3-glycidyloxypropyl)trimethoxysilane (GPTMS); (2) cystamine; (3) 2-bromoisobutyryl bromide (BIBB); (4) (N-isopropylacrylamide)-co-methacrylic acid (NIPAM)/hydroxy ethyl methacrylate (HEMA); (5) DOX-loading at low temperature; (6) cytotoxicity assays

4.2.4. Nitrogen Adsorption/Desorption

In order to evaluate nanoparticles porosity and surface specification, the parameters, including Brunauer-Emmett-Teller (BET) surface area (SBET), mean pore diameter (dp), and cumulative pore volume (Vp) of the MSN and MSN-S-S-PNIPAM were measured by the nitrogen adsorption-desorption method (32).

Mesoporous silica nanoparticles present the typical type IV curve based on the International Union of Pure and Applied Chemistry (IUPAC) nomenclature (Figure 5). In the isotherm of naked MSNs, a well-defined H1-type hysteresis loop with a sharp capillary condensation step at P/P0 of 0.3 - 0.6 shows a typical characteristic of well-ordered mesoporous compounds with cylindrical channels. It can be concluded that after all the modification steps, the nature of mesoporous nanoparticles is preserved well (33).

As depicted in Figure 5, MSN-S-S-PNIPAM adsorbed lesser gas volume, affecting the lower level of the hysteresis loop. Hence, the nanoparticles are partially occupied by the polymer and still have sufficient space for drug loading.

Brunauer-Emmett-Teller surface area, Vp, and dp of

MCM-41 were $939 \text{ m}^2\text{g}^{-1}$, $0.94 \text{ cm}^3\text{g}^{-1}$, and 2.4 nm. After capping the MSNs with thermosensitive polymers, these factors decreased dramatically to $596 \text{ m}^2\text{g}^{-1}$, $0.68 \text{ cm}^3\text{g}^{-1}$, and 2.1 nm. This outcome suggests that PNIPAM can be found in the interior pores and the exterior surface.

4.2.5. Thermogravimetric Analysis and Differential Scanning Calorimetry Analysis

Figure 6 revealed the TGA profiles of MSN, MSN-BIBB, and MSN-S-S-PNIPAM. The TGA results verified the successful modification of MSNs with PNIPAM. Samples were heated to 600°C under the N_2 atmosphere. In the TGA curve of MSN, 3% weight loss occurred at a temperature under 150°C , related to the removal of physically adsorbed water. In the thermogram of MSN-BIBB and MSN-S-S-PNIPAM, the removing adsorbed water was observed in the range of $25 - 100^\circ\text{C}$. In the curve of MSN-BIBB, the grafted functional groups' degradation was observed in the region from 250 to 300°C . Compared to MSN-BIBB, the extra weight loss of MSN-S-S-PNIPAM occurred at around $\sim 330^\circ\text{C}$; (about 20% of total weight), which is attributed to the decomposition of the thermosensitive polymer. This mass reduction was

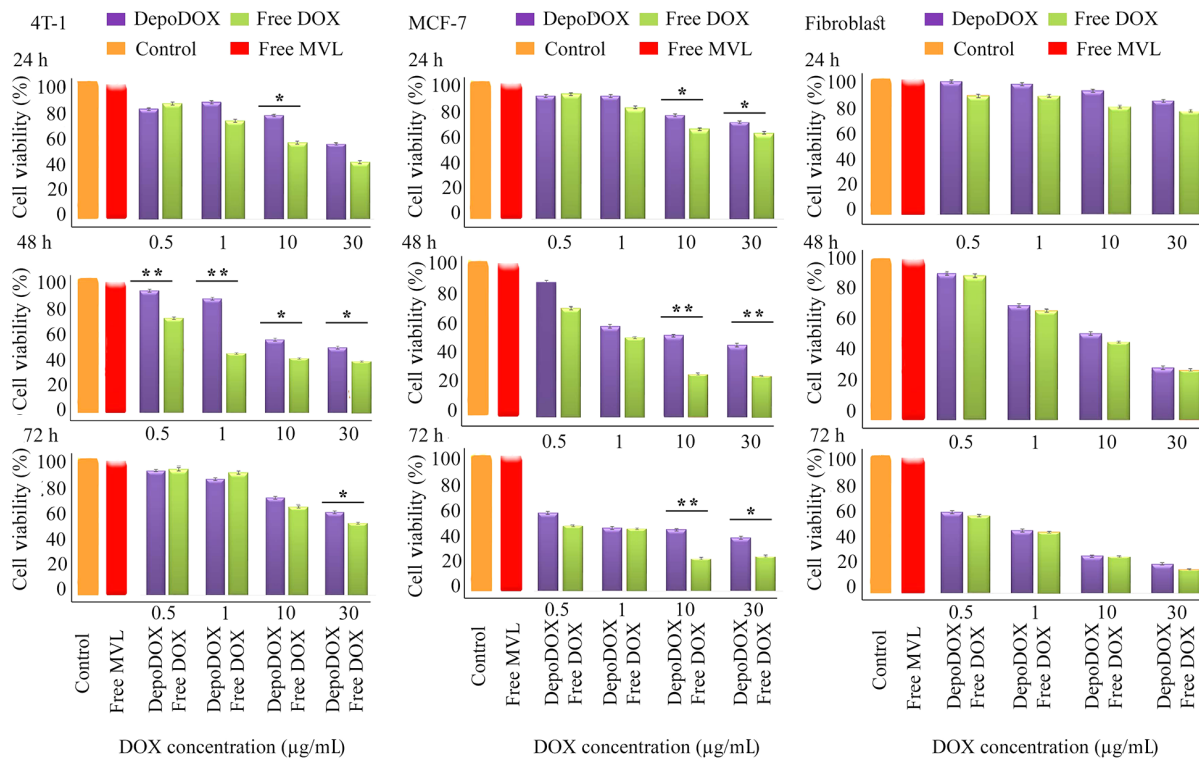


Figure 3. Fourier transform infrared spectra (FTIR) spectra of different steps of synthesizing mesoporous silica nanoparticle (MSN)-S-S-poly(N-isopropylacrylamide) (PNIPAM)

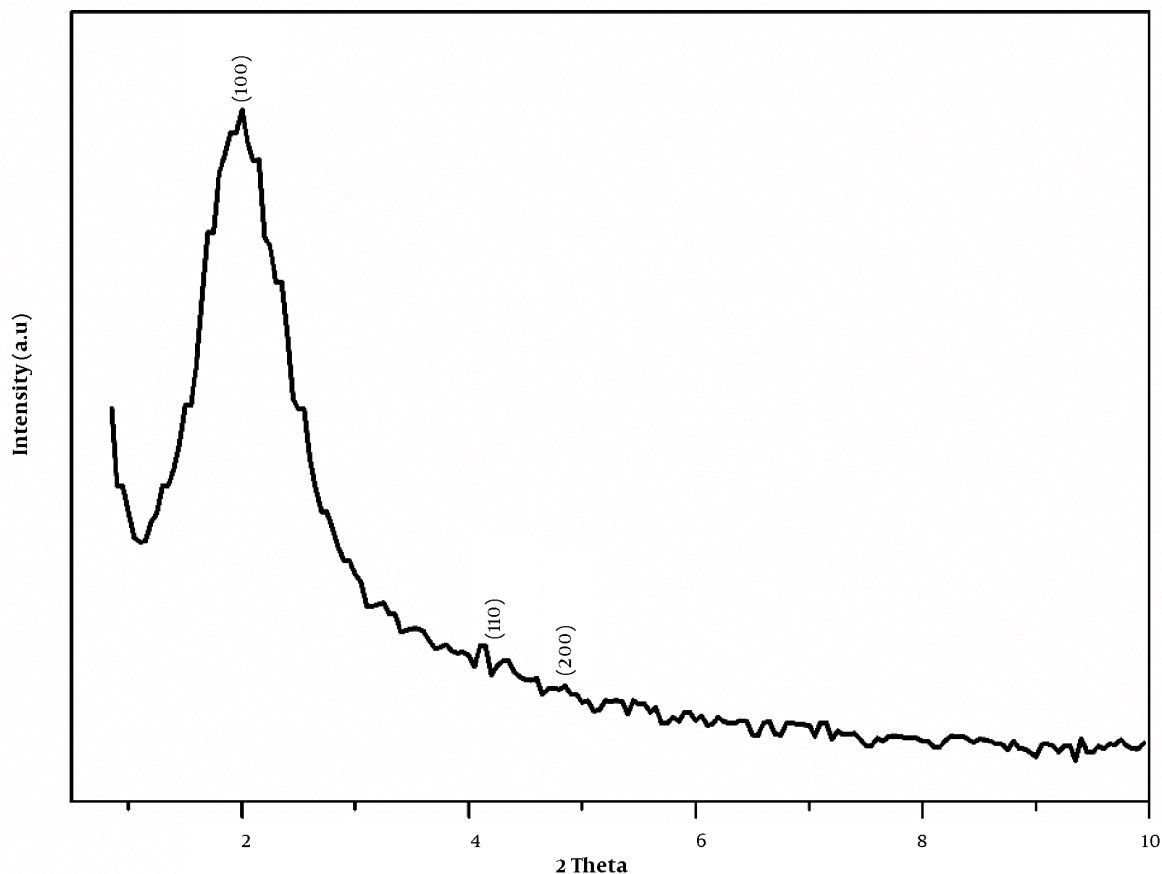


Figure 4. X-ray diffraction (XRD) pattern of mesoporous silica nanoparticle (MSN) (Mobil Composition of Matter No. 41 (MCM-41))

considered equivalent to the coated PNIPAM shell.

Differential scanning calorimetry test of the MSN-S-S-PNIPAM solution was carried out in deionized water to evaluate the phase transition behavior of the PNIPAM shell (Figure 7). It was observed that the heating curve of PNIPAM attached MSNs showed a phase-transition temperature at 39°C that was more than the LCST of pure PNIPAM. Compared to the LCST of neat PNIPAM (about 32°C), the endothermic peak values of PNIPAM might be affected by the HEMA monomer in the structure of the thermo-responsive shell.

4.2.6. Transmission Electron Microscopy Analysis

Transmission electron microscopy images of Figure 8 illustrated a uniform and spherical shape (toward bean-shaped) of mesoporous nanoparticles with an average size of around 150 nm. The MSNs consist of a series of hexagonal parallel channels. Moreover, in Figure 8A, the mesoporous structure with a pore diameter of 2.5 nm can

be clearly distinguished. In the TEM image of MSN-S-S-PNIPAM, the core-shell structure is clearly seen due to the presence of the PNIPAM layer. The distinct grey shell-like layer has a 3 - 6 nm diameter. Also, based on the pictures, the structure of MSNs did not decompose and retain the original size and diameter.

4.2.7. In Vitro Drug Loading and Release Profile

The drug loading content (DLC) and EE of DOX into MSNs carriers were investigated by the UV absorbance method (Table 1).

By increasing DOX to nanoparticle polymer-coated ratio from 0.5: 1 to 2: 1, the DLC % of MSNs increased from 24% to 44%, while the EE decreased from 48% to 22% due to the saturation adsorption of MSNs with the drug molecules. Considering the amount of DOX waste, the optimum drug: Nanoparticle ratio was found to be 1.5: 1. At this ratio, the average drug loading content and encapsulation efficacy were reported as 42% and 29.5%.

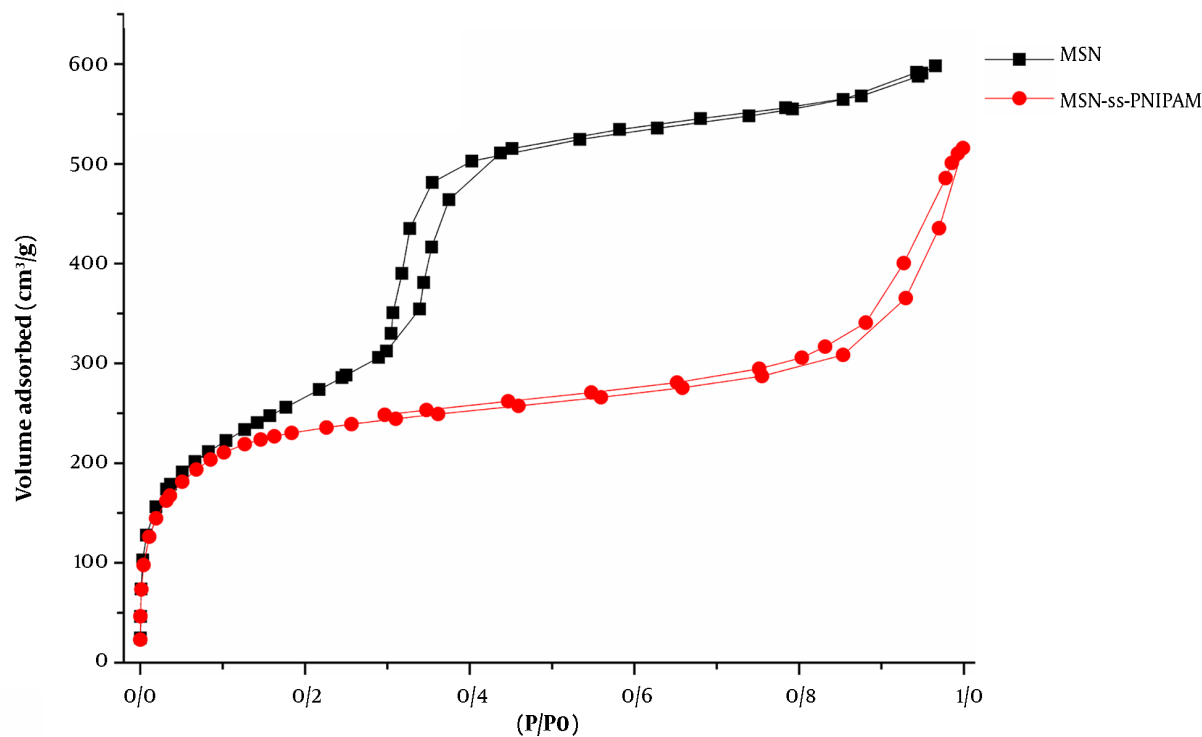


Figure 5. Nitrogen adsorption/desorption of the mesoporous silica nanoparticle (MSN) and MSN-S-S-poly(N-isopropylacrylamide) (PNIPAM) components

Table 1. Drug Loading Capacity and Encapsulation Efficiency of Doxorubicin (DOX)-Mesoporous Silica Nanoparticle (MSN)-S-S-Poly(N-isopropylacrylamide) (PNIPAM)

Doxorubicin: Polymer Ratio	Encapsulation Efficiency (%)	Drug Loading Content (%)
0.5:1	48	24
1:1	35.4	36
1.5:1	29.5	42
2:1	22	44

4.2.8. Release Study

As shown in Figure 9, the drug release profiles of DOX-MSN-S-S-PNIPAM with or without the addition of DTT at different temperatures were measured. At first glance, it is obvious that both temperature and DTT have a synergistic impact on controlling DOX release from the nanoparticles, confirming the double responsive release of mesoporous nanoparticles. However, these dual stimuli-responsive MSNs show a stronger release rate dependence on temperature (i.e., a more significant difference between 25°C and 41°C).

The initial burst release of the drug occurred within 2 h, which 12% and 15% of DOX were released at 25°C and 41°C

with the absence of DTT in release media, while these numbers decreased to 25% and 47% at 25°C and 41°C in the presence of DTT. The physical adsorption of the DOX molecules might have an important role in the burst release.

During 12 h, the cumulative release amount of DOX was 30.5% at 41°C and 18% at 25°C in the absence of DTT. Adding 20 mM of DTT accelerated the release of DOX to 69% at 41°C and 53% at 25°C.

As mentioned in the introduction, PNIPAM, a well-known thermosensitive polymer, acts as a gatekeeper of drug transmission. Hence, below LCST, the long chains of PNIPAM stretch because of the formation of hydrogen bonds between polymer and water, so the polymers inhibit the drug release. Above its LCST, polymers start to shrink and dehydrate, which could lead to decreasing the gap between polymer chains and shorten the release path, so the entrapped DOX could be quickly released (34). The DOX release also depends on the redox process. According to reports, the existence of glutathione plays a key role in the redox targeted delivery due to its higher concentration in cancer cells (35). The DTT attendance in the release medium is similar to the presence of glutathione. The disulfide bonds were broken down by DTT, and the PNIPAM was detached; thus, the channels of MSNs were opened,

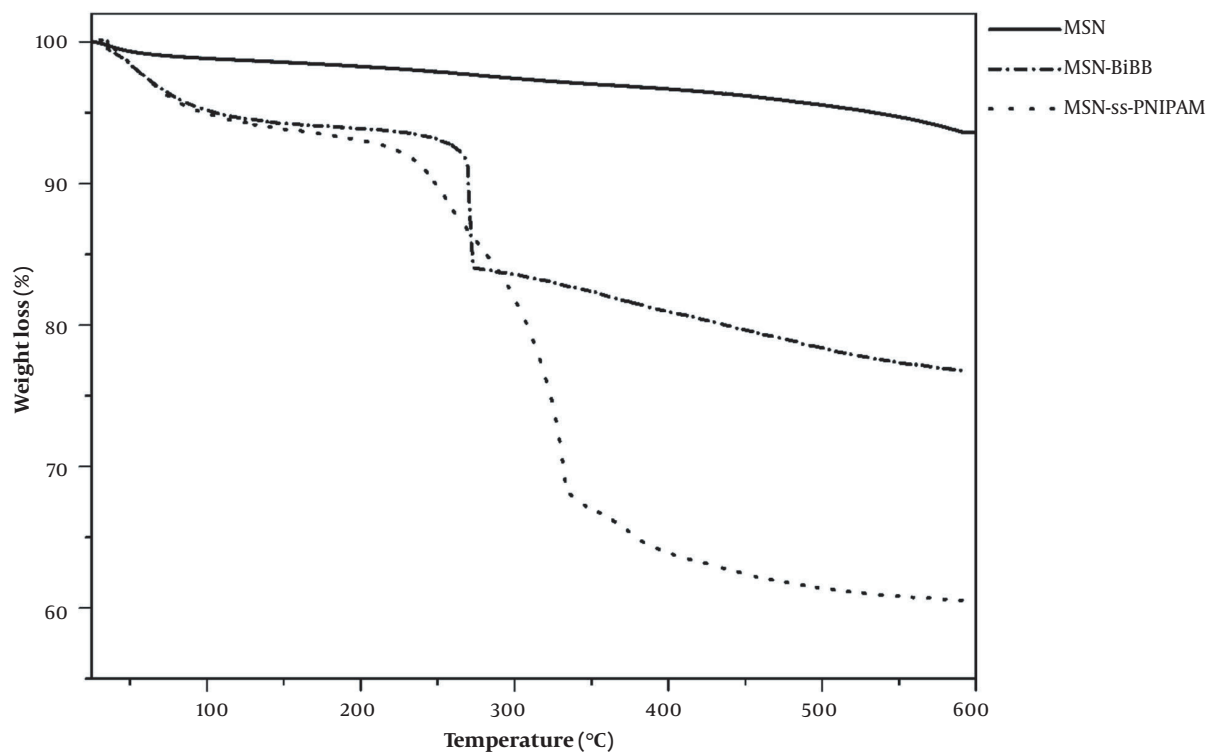


Figure 6. Thermogravimetric analysis (TGA) curves of mesoporous silica nanoparticle (MSN), MSN-2-bromoisobutryl bromide (BiBB), and MSN-S-S-poly(N-isopropylacrylamide) (PNIPAM)

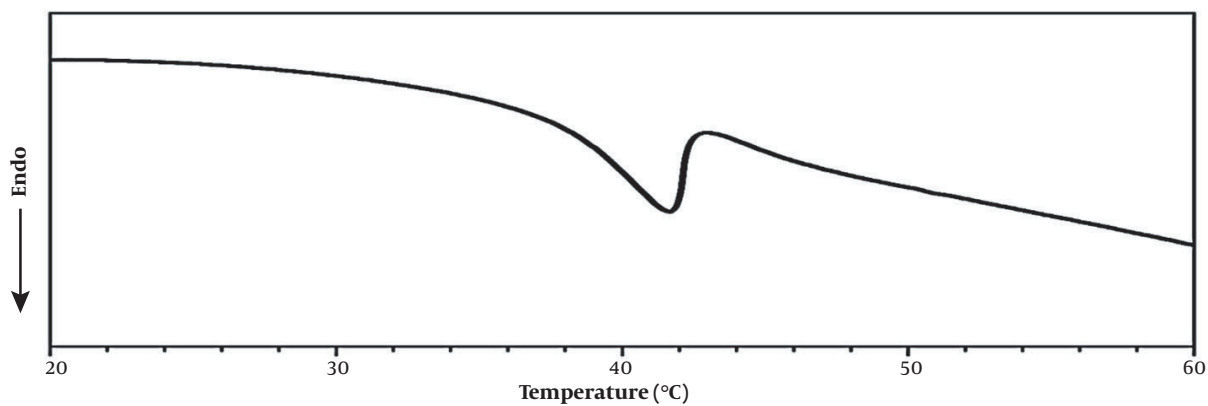


Figure 7. Differential scanning calorimetry measurement of the mesoporous silica nanoparticle (MSN)-S-S-poly(N-isopropylacrylamide) (PNIPAM)

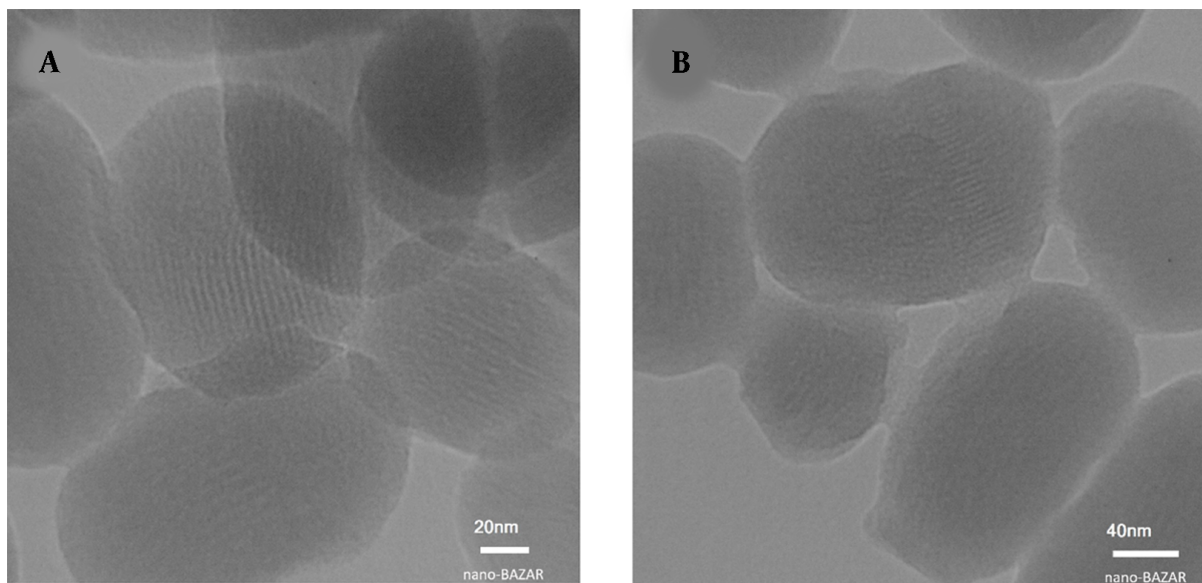


Figure 8. Transmission electron microscopy images of A, mesoporous silica nanoparticle (MSN) and; B, MSN-S-S-poly(N-isopropylacrylamide) (PNIPAM)

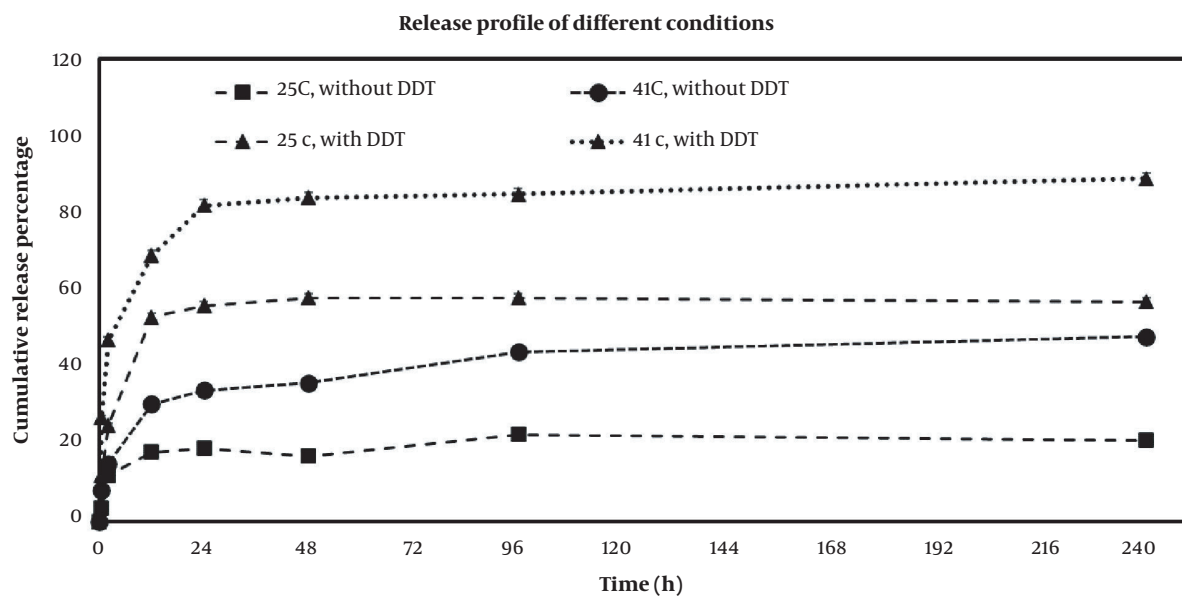


Figure 9. In vitro release profile of doxorubicin (DOX) from DOX-mesoporous silica nanoparticle (MSN)-S-S-poly(N-isopropylacrylamide) (PNIPAM) in two temperatures of 25°C and 41°C with and without reducing agent of dithiothreitol (DTT)

and the release of DOX molecules was accelerated remarkably.

4.2.9. In Vitro Cytotoxicity Assays

Different cell models derived from mammalian cells are used as a suitable method to analyze the biocompatibility and cytotoxicity of chemotherapeutic agent nanoformulations. Michigan Cancer Foundation-7 cells, one of the breast cancer cell lines used as a cell model to determine their cell viability and proliferation against different samples of both groups (free DOX and DOX loaded NPs). This assay was measured by using tetrazolium salt MTT (30).

Generally, the increment of the DOX concentrations results in the cytotoxicity elevation of both formulations. A significant reduction in cell population was observed in the MCF-7 cells exposed to DOX-MSN-S-S-PNIPAM compared to free DOX. The difference between the viability of the cells treated with nano-formulations and the free drug increased as the drug concentration increased.

Many researchers tried to explain these differences as a result of the cellular uptake mechanisms of the drug. Free DOX can easily pass through the cell membrane and enter its active site. As mentioned, DOX molecules were pumped out of the cells via P-gp systems, leading to reduced chemotherapy efficacy. On the other hand, the internalization of DOX-loaded nanoparticles into cells occurs through passive endocytosis. Thus, the cellular uptake of DOX was enhanced notably (36).

Furthermore, as Figure 10 shows, the cell viability of MCF-7 cells in $0.5 \mu\text{g.mL}^{-1}$ was about $\sim 71\%$ in DOX loaded MSN-S-S-PNIPAM and $\sim 75\%$ in free DOX, while in $10 \mu\text{g.mL}^{-1}$ it was $\sim 22\%$ and $\sim 32\%$, respectively.

So it can be concluded that at the range of $0.5 - 10 \mu\text{g.mL}^{-1}$, both DOX and DOX loaded MSN-S-S-PNIPAM illustrated concentration-dependent toxicity against cells.

All data were presented as mean \pm SD. Parametric variables were analyzed using a one-way analysis of variance (ANOVA) followed by Tukey's post-hoc test. All statistical analyses were performed in SPSS 18 (SPSS Inc., Chicago, IL, USA). P values less than 0.05 were considered significant for all statistical tests.

4.3. Conclusions

The nanoparticles were used for the controlled release of DOX to cancer cells.

In this study, thermosensitive PNIPAM chains grafted to the mesoporous silica, a stimuli-responsive drug delivery platform, were developed. In addition, the nanoparticles, including disulfide bonds, were used for grafting the polymeric nanoparticles to have a dual-responsive system.

Nanoparticles, including a grey shell-like layer with a diameter of 3-6 nm on the surface, were developed by grafting NIPAM on MSN.

To find the best condition for drug loading and encapsulation of DOX into MSNs carriers, different concentrations of the DOX were used. In optimum conditions, with a ratio of 1.5: 1 of DOX to the nanoparticle, the DLC% was 42%, while the EE was 29.5%. In comparison, the lowest EE was achieved with a ratio of 2: 1.

To evaluate DOX-MSN-S-S-PNIPAM nanoparticles' responsibility, the drug release profiles in the presence and absence of DTT at 25°C and 41°C were evaluated. Doxorubicin release was 63% more at 41°C and the presence of DTT, in comparison to 25°C and absence of DTT at 24 h, confirmed the double responsive release of mesoporous nanoparticles. These results showed that DOX-MSN-S-S-PNIPAM nanoparticles are dual stimuli-responsive.

According to the MTT test results, these controlled release DOX-MSN-S-S-PNIPAM nanoparticles have shown more efficient cytotoxicity compared to DOX against the MCF-7 cell line. This effect may be due to the cell uptake of MSN-S-S-PNIPAM, which should be evaluated by further studies. Regarding the beneficial behavior of the nanoparticles, it could be concluded that MSN-S-S-PNIPAM could be an interesting candidate for the smart delivery of DOX to cancer cells.

Footnotes

Authors' Contribution: Study concept and design: Mohammad Erfan, Rassoul Dinarvand, Arash Mahboubi and Yalda Hosseinzadeh Ardakani; acquisition of data: Arash Mahboubi and S. Mostafa Ebrahimi; analysis and interpretation of data: Arash Mahboubi, S. Mostafa Ebrahimi and Mahtab Rashed; drafting of the manuscript: Rassoul Dinarvand, Arash Mahboubi, Mahdieh Karamat Iradmousa and Yousef Fatahi; critical revision of the manuscript for important intellectual content: Arash Mahboubi and S. Mostafa Ebrahimi; statistical analysis: Saeed Bahadorikhalili and Reza Bafkary.

Conflict of Interests: The authors declare that they have no conflict of interests.

Funding/Support: This study was supported in part by Shahid Beheshti University of Medical Sciences (grant number 31891).

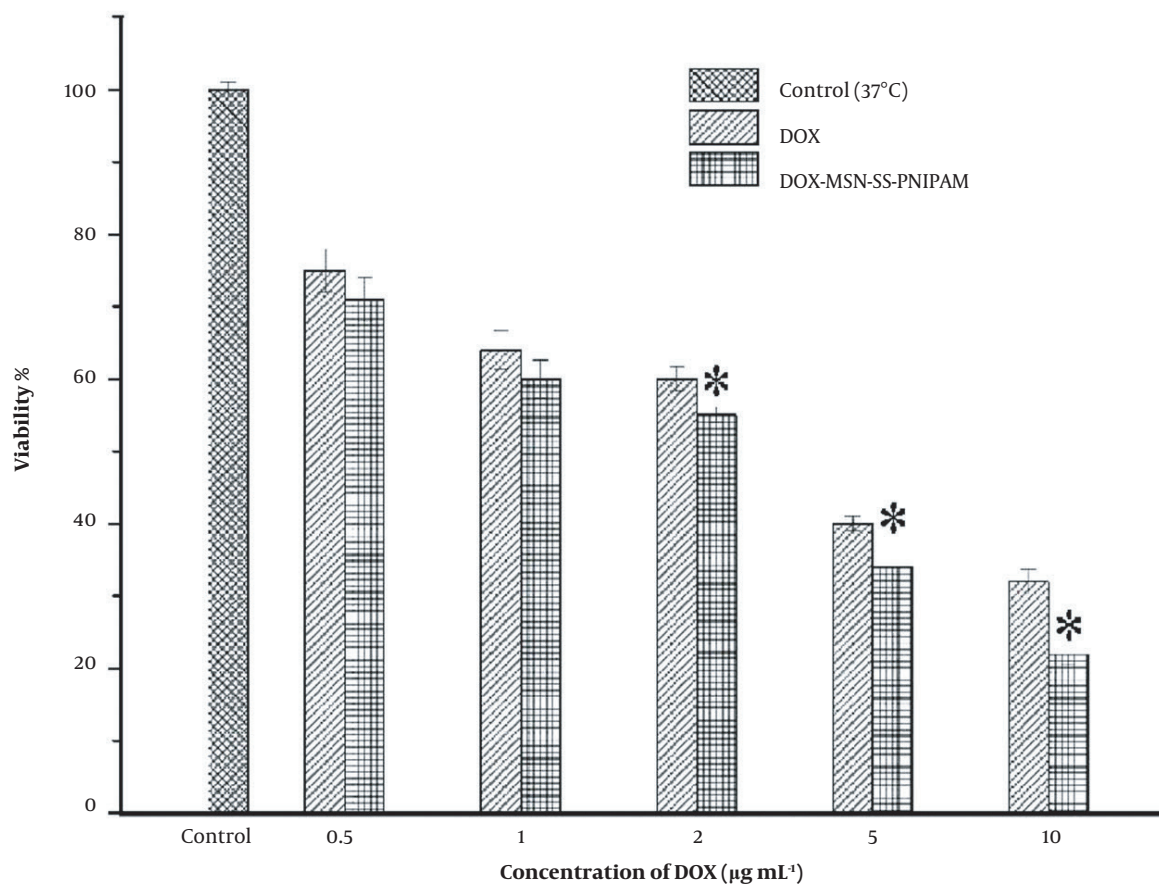


Figure 10. The cytotoxicity of doxorubicin (DOX) and DOX-mesoporous silica nanoparticle (MSN)-S-S-poly(N-isopropylacrylamide) (PNIPAM) in different concentrations against Michigan Cancer Foundation-7 (MCF-7) cell line. Results were expressed as mean \pm SD (n = 5); significance was calculated by ANOVA (* P \leq 0.05).

References

1. Tacar O, Sriamornsak P, Dass CR. Doxorubicin: an update on anticancer molecular action, toxicity and novel drug delivery systems. *J Pharm Pharmacol.* 2013;**65**(2):157-70. [PubMed ID: 23278683]. <https://doi.org/10.1111/j.2042-7158.2012.01567.x>.
2. Di Martino A, Kucharczyk P, Capakova Z, Humpolicek P, Sedlarik V. Chitosan-based nanocomplexes for simultaneous loading, burst reduction and controlled release of doxorubicin and 5-fluorouracil. *Int J Biol Macromol.* 2017;**102**:613-24. [PubMed ID: 28431942]. <https://doi.org/10.1016/j.ijbiomac.2017.04.004>.
3. Christowitz C, Davis T, Isaacs A, van Niekerk G, Hattingh S, Engelbrecht AM. Mechanisms of doxorubicin-induced drug resistance and drug resistant tumour growth in a murine breast tumour model. *BMC Cancer.* 2019;**19**(1):757. [PubMed ID: 31370818]. [PubMed Central ID: PMC6670209]. <https://doi.org/10.1186/s12885-019-5939-z>.
4. Ye Q, Liu K, Shen Q, Li Q, Hao J, Han F, et al. Reversal of Multidrug Resistance in Cancer by Multi-Functional Flavonoids. *Front Oncol.* 2019;**9**:487. [PubMed ID: 31245292]. [PubMed Central ID: PMC6581719]. <https://doi.org/10.3389/fonc.2019.00487>.
5. Mansoori B, Mohammadi A, Davudian S, Shirjang S, Baradaran B. The Different Mechanisms of Cancer Drug Resistance: A Brief Review. *Adv Pharm Bull.* 2017;**7**(3):339-48. [PubMed ID: 29071215]. [PubMed Central ID: PMC5651054]. <https://doi.org/10.1517/apb.2017.041>.
6. Li H, Zhang JZ, Tang Q, Du M, Hu J, Yang D. Reduction-responsive drug delivery based on mesoporous silica nanoparticle core with crosslinked poly(acrylic acid) shell. *Mater Sci Eng C Mater Biol Appl.* 2013;**33**(6):3426-31. [PubMed ID: 23706230]. <https://doi.org/10.1016/j.msec.2013.04.033>.
7. Chang B, Sha X, Guo J, Jiao Y, Wang C, Yang W. Thermo and pH dual responsive, polymer shell coated, magnetic mesoporous silica nanoparticles for controlled drug release. *J Mater Chem.* 2011;**21**(25). <https://doi.org/10.1039/c1jm10631g>.
8. Beck JS, Vartuli JC, Roth WJ, Leonowicz ME, Kresge CT, Schmitt KD, et al. A new family of mesoporous molecular sieves prepared with liquid crystal templates. *J Am Chem Soc.* 1992;**114**(27):10834-43. <https://doi.org/10.1021/ja00053a020>.
9. Mohseni M, Gilani K, Mortazavi SA. Preparation and characterization of rifampin loaded mesoporous silica nanoparticles as a potential system for pulmonary drug delivery. *Iran J Pharm Res.* 2015;**14**(1):27-34. [PubMed ID: 25561909]. [PubMed Central ID: PMC4277616].
10. Rascol E, Pisani C, Dorandeu C, Nyalosaso JL, Charnay C, Daurat M, et al. Biosafety of Mesoporous Silica Nanoparticles. *Biomimetics (Basel).* 2018;**3**(3). [PubMed ID: 31105244]. [PubMed Central ID: PMC6352691]. <https://doi.org/10.3390/biomimetics3030022>.
11. Hu X, Hao X, Wu Y, Zhang J, Zhang X, Wang PC, et al. Multifunctional hybrid silica nanoparticles for controlled doxorubicin loading and release with thermal and pH dually response. *J Mater*

- Chem B.* 2013;**1**(8):1109–18. [PubMed ID: 2354391]. [PubMed Central ID: PMC3609667]. <https://doi.org/10.1039/C2TB00223j>.
12. Florek J, Caillard R, Kleitz F. Evaluation of mesoporous silica nanoparticles for oral drug delivery - current status and perspective of MSNs drug carriers. *Nanoscale.* 2017;**9**(40):15252–77. [PubMed ID: 28984885]. <https://doi.org/10.1039/c7nr05762h>.
 13. Tian Y, Kong Y, Li X, Wu J, Ko AC, Xing M. Light- and pH-activated intracellular drug release from polymeric mesoporous silica nanoparticles. *Colloids Surf B Biointerfaces.* 2015;**134**:147–55. [PubMed ID: 26188470]. <https://doi.org/10.1016/j.colsurfb.2015.04.069>.
 14. Qiu K, He C, Feng W, Wang W, Zhou X, Yin Z, et al. Doxorubicin-loaded electrospun poly(L-lactic acid)/mesoporous silica nanoparticles composite nanofibers for potential postsurgical cancer treatment. *J Mater Chem B.* 2013;**1**(36):4601–11. [PubMed ID: 32261203]. <https://doi.org/10.1039/c3tb20636j>.
 15. Adhikari C, Chakraborty A. Synthesis, Characterization and Application of Zeolitic Imidazole Framework-Mesoporous Silica Nanospheres Composite: A Hybrid Porous Composite for Drug Delivery. *J Phys Conf Ser.* 2020;**1531**(1). <https://doi.org/10.1088/1742-6596/1531/1/012095>.
 16. Huang Y, Zhao X, Zu Y, Wang L, Deng Y, Wu M, et al. Enhanced Solubility and Bioavailability of Apigenin via Preparation of Solid Dispersions of Mesoporous Silica Nanoparticles. *Iran J Pharm Res.* 2019;**18**(1):168–82. [PubMed ID: 31089353]. [PubMed Central ID: PMC6487423].
 17. Heidarli E, Dadashzadeh S, Haeri A. State of the Art of Stimuli-Responsive Liposomes for Cancer Therapy. *Iran J Pharm Res.* 2017;**16**(4):1273–304. [PubMed ID: 29552041]. [PubMed Central ID: PMC5843293].
 18. Tian Z, Yu X, Ruan Z, Zhu M, Zhu Y, Hanagata N. Magnetic mesoporous silica nanoparticles coated with thermo-responsive copolymer for potential chemo- and magnetic hyperthermia therapy. *Microporous Mesoporous Mater.* 2018;**256**:1–9. <https://doi.org/10.1016/j.micromeso.2017.07.053>.
 19. Rao NV, Ko H, Lee J, Park JH. Recent Progress and Advances in Stimuli-Responsive Polymers for Cancer Therapy. *Front Bioeng Biotechnol.* 2018;**6**:110. [PubMed ID: 30159310]. [PubMed Central ID: PMC6104418]. <https://doi.org/10.3389/fbioe.2018.00110>.
 20. Sharif Makhmalzadeh B, Salimi A, Niroomand A. Loratadine-Loaded Thermoresponsive Hydrogel: Characterization and Ex-vivo Rabbit Cornea Permeability Studies. *Iran J Pharm Res.* 2018;**17**(2):460–9. [PubMed ID: 29881404]. [PubMed Central ID: PMC5985164].
 21. Ugazio E, Gastaldi L, Brunella V, Scalapone D, Jadhav SA, Oliaro-Bosso S, et al. Thermoresponsive mesoporous silica nanoparticles as a carrier for skin delivery of quercetin. *Int J Pharm.* 2016;**511**(1):446–54. [PubMed ID: 27421910]. <https://doi.org/10.1016/j.ijpharm.2016.07.024>.
 22. Gui R, Wang Y, Sun J. Encapsulating magnetic and fluorescent mesoporous silica into thermosensitive chitosan microspheres for cell imaging and controlled drug release in vitro. *Colloids Surf B Biointerfaces.* 2014;**113**:1–9. [PubMed ID: 24060924]. <https://doi.org/10.1016/j.colsurfb.2013.08.015>.
 23. Conzatti G, Cavalie S, Combes C, Torrisani J, Carrere N, Tourrette A. PNIPAM grafted surfaces through ATRP and RAFT polymerization: Chemistry and bioadhesion. *Colloids Surf B Biointerfaces.* 2017;**151**:143–55. [PubMed ID: 27992845]. <https://doi.org/10.1016/j.colsurfb.2016.12.007>.
 24. Chen J, Liu M, Gong H, Huang Y, Chen C. Synthesis and self-assembly of thermoresponsive PEG-b-PNIPAM-b-PCL ABC triblock copolymer through the combination of atom transfer radical polymerization, ring-opening polymerization, and click chemistry. *J Phys Chem B.* 2011;**115**(50):14947–55. [PubMed ID: 22082119]. <https://doi.org/10.1021/jp208494w>.
 25. Lin JT, Liu ZK, Zhu QL, Rong XH, Liang CL, Wang J, et al. Redox-responsive nanocarriers for drug and gene co-delivery based on chitosan derivatives modified mesoporous silica nanoparticles. *Colloids Surf B Biointerfaces.* 2017;**155**:41–50. [PubMed ID: 28407530]. <https://doi.org/10.1016/j.colsurfb.2017.04.002>.
 26. Asadpour E, Sadeghnia HR, Ghorbani A, Boroushaki MT. Effect of zirconium dioxide nanoparticles on glutathione peroxidase enzyme in PC12 and n2a cell lines. *Iran J Pharm Res.* 2014;**13**(4):1141–8. [PubMed ID: 25587301]. [PubMed Central ID: PMC4232778].
 27. Nhavene E, Andrade G, Faria J, Gomes D, Sousa E. Biodegradable Polymers Grafted onto Multifunctional Mesoporous Silica Nanoparticles for Gene Delivery. *ChemEngineering.* 2018;**2**(2). <https://doi.org/10.3390/chemengineering2020024>.
 28. Zhang R, Liu Z, Luo Y, Xu F, Chen Y. Tri-stimuli responsive carbon nanotubes covered by mesoporous silica graft copolymer multifunctional materials for intracellular drug delivery. *J Ind Eng Chem.* 2019;**80**:431–43. <https://doi.org/10.1016/j.jiec.2019.08.023>.
 29. Yu E, Galiana I, Martinez-Manez R, Stroev P, Marcos MD, Aznar E, et al. Poly(N-isopropylacrylamide)-gated Fe₃O₄/SiO₂ core shell nanoparticles with expanded mesoporous structures for the temperature triggered release of lysozyme. *Colloids Surf B Biointerfaces.* 2015;**135**:652–60. [PubMed ID: 26335056]. <https://doi.org/10.1016/j.colsurfb.2015.06.048>.
 30. Chen K, Chang C, Liu Z, Zhou Y, Xu Q, Li C, et al. Hyaluronic acid targeted and pH-responsive nanocarriers based on hollow mesoporous silica nanoparticles for chemo-photodynamic combination therapy. *Colloids Surf B Biointerfaces.* 2020;**194**:111166. [PubMed ID: 32521461]. <https://doi.org/10.1016/j.colsurfb.2020.111166>.
 31. Vaysipour S, Rafiee Z, Nasr-Esfahani M. Synthesis and characterization of copper (II)-poly(acrylic acid)/MCM-41 nanocomposite as a novel mesoporous solid acid catalyst for the one-pot synthesis of polyhydroquinoline derivatives. *Polyhedron.* 2020;**176**. <https://doi.org/10.1016/j.poly.2019.114294>.
 32. Glotov A, Vutolkina A, Pimerzin A, Nedolivko V, Zasyalov G, Stytsenko V, et al. Ruthenium Catalysts Templated on Mesoporous MCM-41 Type Silica and Natural Clay Nanotubes for Hydrogenation of Benzene to Cyclohexane. *Catalysts.* 2020;**10**(5). <https://doi.org/10.3390/catal10050537>.
 33. Feng D, Feng Y, Li P, Zang Y, Wang C, Zhang X. Modified mesoporous silica filled with PEG as a shape-stabilized phase change materials for improved thermal energy storage performance. *Microporous Mesoporous Mater.* 2020;**292**. <https://doi.org/10.1016/j.micromeso.2019.109756>.
 34. Guo F, Li G, Ma S, Zhou H, Yu X. Dual-responsive nanocarriers from star shaped poly(N-isopropylacrylamide) coated mesoporous silica for drug delivery. *Int J Polym Mater.* 2019;**69**(18):1178–86. <https://doi.org/10.1080/00914037.2019.1683555>.
 35. Li X, He G, Jin H, Tao J, Li X, Zhai C, et al. Dual-Therapeutics-Loaded Mesoporous Silica Nanoparticles Applied for Breast Tumor Therapy. *ACS Appl Mater Interfaces.* 2019;**11**(50):46497–503. [PubMed ID: 31738505]. <https://doi.org/10.1021/acsami.9b16270>.
 36. Kamba AS, Ismail M, Ibrahim TA, Zakaria ZA, Gusau LH. In vitro ultrastructural changes of MCF-7 for metastasis bone cancer and induction of apoptosis via mitochondrial cytochrome C released by CaCO₃/Dox nanocrystals. *Biomed Res Int.* 2014;**2014**:391869. [PubMed ID: 25028650]. [PubMed Central ID: PMC4084513]. <https://doi.org/10.1155/2014/391869>.